JACS
JOURNAL OF THE AMERICAN CHEMICAL SOCIETY
pubs.acs.org/JACS
Communication

Two Blatter Radicals Face-to-Face: A Constrained Diradical Architecture

Paulina Bartos, Dominika Pomikło, Kadin B. Sorenson, Oleksandr Hietsoi, Andrienne C. Friedli, and Piotr Kaszyński*

Cite This: J. Am. Chem. Soc. 2025, 147, 125−129
Read Online
ACCESS | Metrics & More | Article Recommendations | Supporting Information

ABSTRACT: Cofacial arrangement of two Blatter radicals enforced by the *peri*-naphthalene scaffold represents a new approach to stable diradicals with strong through-space interactions. Two stereoisomers of the naphthalene-diradicals, *anti* and *syn*, are investigated by XRD, VT-EPR, UV−vis, electrochemical, kinetic, and DFT methods. In solutions, both stereoisomers exist as open-shell singlets with $\Delta E_{S\text{-}T}$ = −3.1 and −3.8 kcal mol^{-1}, respectively. The *anti* isomer was resolved into enantiomers and converts to *syn* with $\Delta G^{\ddagger}_{298}$ = 23.6(8) kcal mol^{-1}.

Stable diradicals[1] and diradicaloids[2] are of interest for fundamental science and for the development of functional materials.[3] A combination of the readily thermally accessible high-spin states, redox properties, and low excitation energies are attractive for applications, such as near-IR dyes,[4] nonlinear optics,[5] sensors,[6] and singlet fission[7] in photovoltaic devices. The recent focus in investigation of such open-shell systems is on derivatives[8] of the Blatter radical[9] (Figure 1), which offers high stability, structural versatility, and electronic tunability.

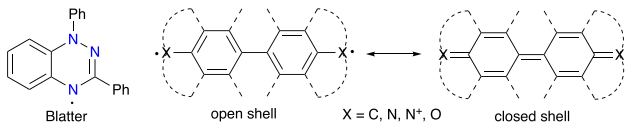

Figure 1. Left: Blatter radical. Right: Generic open-shell and closed-shell structures for diradicaloid molecules. For a list of examples, see ref 10.

A typical molecular design of diradicals/diradicaloids[11] involves communication through the π system and takes advantage of the interplay between aromaticity/antiaromaticity and closed- *vs* open-shell structures in extended polycyclic systems[2b,12] or topology[13] of the connectivity of two radicals (Figure 1). An attractive alternative to the covalent bond approach is through space interaction[14] of π-delocalized radicals. To date, there are very few diradicals with such through-space interactions and they are mainly based on the [2,2]paracyclophane with 3.03 Å interdeck separation (phenylcarbenes **A**,[15] nitroxides **B**,[16] and fluorenyls **C** and **D**,[16] Figure 2), ferrocene[17] with 3.3 Å Cp separation (verdazyl **E**),[18] and phenanthrene (**F**) with angular orientation of the radical units in equilibrium with the closed-shell zwitterion form.[19] Among the three scaffolds, only [2,2]paracyclophane can effectively support axially chiral diradicals, but their isolation has not been attempted so far.

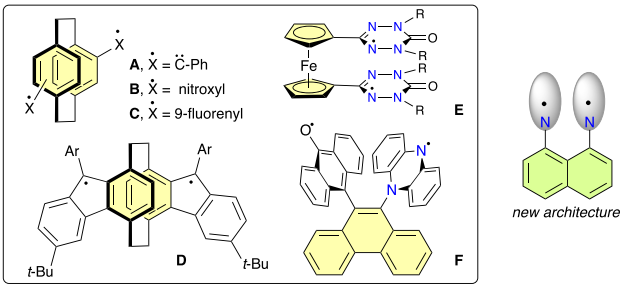

Figure 2. In the box: Previously investigated diradicals were based on the [2.2]paracyclophane (**A**−**D**), ferrocene (**E**), and phenanthrene (**F**) scaffolds. Right: new architecture for cofacial arrangements of two Blatter radicals.

1,8-Disubstituted naphthalene is recognized as an attractive scaffold for imposing tight, cofacial π−π interactions of aromatic systems (the C(1)···C(8) distance: 2.5 Å), which alters their photophysical[20] and redox[20b,21] properties and occasionally leads to conformationally stable enantiomers.[22] So far, naphthalene has not been used for a close, parallel arrangement of two π-delocalized radicals, and the behavior of such π-compressed diradicals remains unknown.

Herein we report a new, highly constrained architecture for open-shell singlet diradicals based on the *peri*-naphthalene scaffold in a cofacial arrangement of two Blatter radicals interacting through space (Figure 2). We isolate two forms of the diradical, **1**-*syn* and **1**-*anti*, determine their molecular structures and kinetics of interconversion, and measure their

Received: November 20, 2024
Revised: December 13, 2024
Accepted: December 17, 2024
Published: December 20, 2024

https://doi.org/10.1021/jacs.4c16500
J. Am. Chem. Soc. 2025, 147, 125−129

S−T energy gaps. The racemic **1**-*anti* is separated into enantiomers, and ECD spectra are measured. Both forms of the diradical undergo oxidation and the cations are analyzed by XRD methods. Experimental data are compared to DFT computational results.

The synthesis of the diradicals followed the recently described azaphilic addition of aryllithiums to benzo[*e*][1,2,4]-trazines.[23] Thus, treatment of 3-phenylbenzo[*e*][1,2,4]triazine (**2**) with 1,8-dilithionaphthalene, generated from 1,8-dibromonaphthalene, led to a mixture of **1**-*syn* and **1**-*anti* diradicals (Scheme 1). The diastereoisomers were separated based on solubility differences and further purified by column chromatography to give 39 and 18% yield of **1**-*syn* and **1**-*anti*, respectively.

Scheme 1. Synthesis of diradicals 1

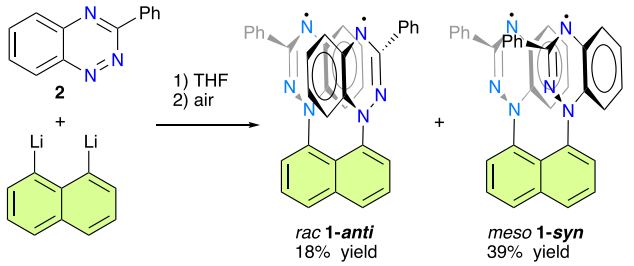

XRD analysis of dark yellow-brown single crystals demonstrated that in **1**-*syn* both nearly planar benzo[*e*][1,2,4]-triazinyls are essentially orthogonal to the naphthalene ring (Figure 3), while mean planes of the heterocycles form an

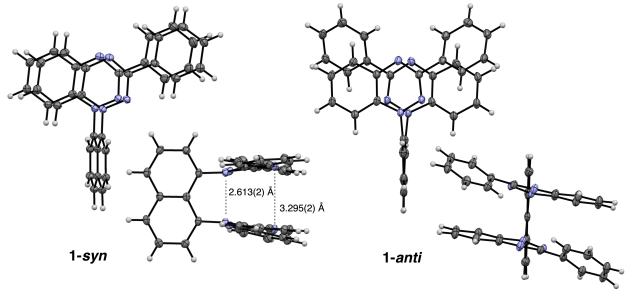

Figure 3. Molecular structures of **1**-*syn* (left) and **1**-*anti* (molecule A, right). Atomic displacement ellipsoids are drawn at the 50% probability level. N atoms are in blue. See text and SI for details.

angle of 13.6° with the distances between N(1)···N(1′) and N(4)···N(4′) nitrogen atoms of 2.613(2) and 3.295(2) Å. Both distances are larger than the separation between the *peri* positions in naphthalene (2.520(3) Å). In **1**-*anti* the heterocyclic fragments in the two independent molecules form a mean angle of 81.4° with the naphthalene ring and 13° (molecule **I**) and 22° (molecule II) angles between them. Consequently, the N(1)···N(1′) separation is 2.590(2) Å in both molecules, while the N(4)···N(4′) distance is 3.174(2) and 3.604(2) Å in molecules I and II, respectively. The proximity of the spin-bearing heterocycles, and the contact between the N(1) atoms N(1′) of about 0.5 Å inside the van der Waals separation, suggest a strong tendency for the singlet GS, but not a covalent bond. Indeed, DFT calculations at the (U)B3LYP/6-311G(d,p) level of theory indicate that this solid-state geometry corresponds to the closed-shell singlet (CSS) state with the calculated N(1)···N(1′) and N(4)···N(4′) distances of 2.587 and 3.525 Å for **1**-*syn* and 2.547 and 3.470 Å for **1**-*anti* conformer, respectively. So far, covalent dimers of Blatter radicals have not been observed, and the two reported related structures result from oxidative N(4)−C(5′) and N(2)−C(5′) coupling.[24]

Further DFT analysis demonstrates that the lowest energy state in each stereoisomer is the open-shell singlet (OSS), which is 4.63 and 4.98 kcal mol^{-1} below the CSS for **1**-*anti* and **1**-*syn*, respectively, and is characterized by greater separation between the N(1)···N(1′) atoms: 2.783 and 2.806 Å, respectively.

DFT calculations indicate that the OSS ground state of **1**-*anti* is more stable than that of the **1**-*syn* isomer, suggesting that the observed dominant **1**-*syn* is a kinetic product. Indeed, heating of a sample of **1**-*syn* at 100 °C (PhCl) for 1.5 h led to a mixture of the two isomers, from which **1**-*anti* and **1**-*syn* were isolated in 67 and 26% yield, respectively. Kinetic measurements of the appearance of **1**-*syn* during thermal equilibration of **1**-*anti* at four temperatures gave activation parameters of $\Delta H^{\ddagger}$ = 24.6(8) kcal mol^{-1} and $\Delta S^{\ddagger}$ = 3.4(12) cal mol^{-1} K^{-1}, which can be assumed to represent the barrier to racemization of enantiomeric **1**-*anti*. The half-life of **1**-*anti* at 65 °C was determined to be 139 min, while the equilibrium ratio of isomers was the same K(*anti*/*syn*) = 1.904(16) within the experimental error at all four temperatures. The latter indicates that the isomer distribution is an entropy-driven process (ΔH = 0.0 kcal mol^{-1} and ΔS = 1.28(2) cal mol^{-1} K^{-1}).

UV−vis measurements revealed a broad, moderately intense absorption band in **1**-*syn* at 622 nm (log ε 3.84) and at 678 nm (log ε 3.78) for **1**-*anti* (Figure 4), consistent with the blue

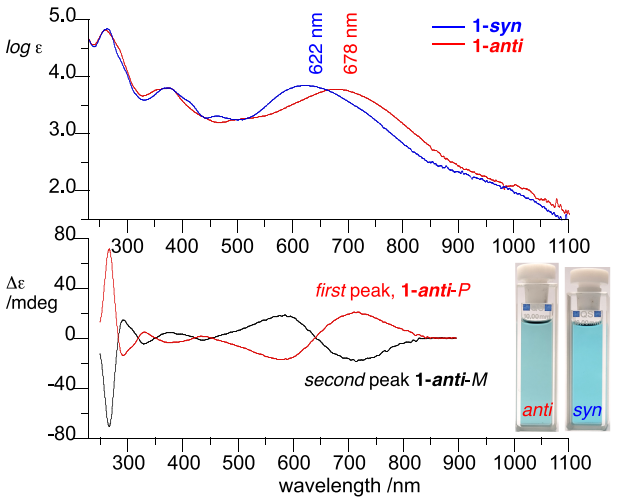

Figure 4. Top: UV−vis spectra for diradical **1**-*anti* (red) and **1**-*syn* (blue) recorded in CH_2Cl_2. Bottom: ECD spectra for the enantiomers of **1**-*anti* in hexane/CH_2Cl_2. The "*first*" and "*second*" labels refer to the order of peaks in the chromatogram with assigned absolute configurations (based on DFT). The inset shows analyzed solutions.

color of their solutions. These bands are significantly red-shifted relative to that in the Blatter radical (λ_{max} = 492 nm) and are due to strong transannular interactions. TD-DFT calculations demonstrated that this intense low energy absorption band is related to the $S_0 \rightarrow S_2$ excitation (calculated at 798 and 790 nm ($f \sim 0.06$), for **1**-*syn* and **1**-*anti*, respectively) and solely due to the HOMO−LUMO excitation

https://doi.org/10.1021/jacs.4c16500
J. Am. Chem. Soc. 2025, 147, 125−129

involving α and β electron manifolds. The $S_0 \rightarrow S_1$ transition is a double-excitation characteristic for diradicals[25] calculated at about 920 nm with $f \sim 0.0001$ in both diradicals **1** and appearing as a low intensity shoulder above 850 nm in the experimental spectra (Figure 4). Notably, while the diradicals **1** in the solid state appear to have closed-shell singlet (CSS) character and form dark brown-yellow crystals, their solutions are blue indicating the dominant open-shell character.[26] Moreover, the blue color associated with the open shell structure of the diradicals persists in solid solutions, even at 77 K. TD-DFT calculations for the CSS diradicals **1** indeed indicated a hypsochromic shift of the HOMO−LUMO transition relative to the OSS forms by about 0.2 eV.[26] A similar CSS−OSS interconversion and two-electron multicenter dimerization in the solid state was reported[18] for diverdazyl **E** (Figure 2).

Variable temperature EPR studies of both diradicals performed in poly(2-isopropenyl-2-oxazoline) solid solutions in the temperature range of 149−370 K revealed increasing intensity of the signal characteristic for a triplet state with monoradical impurities (Figure 5). Zero-field splitting (*zfs*)

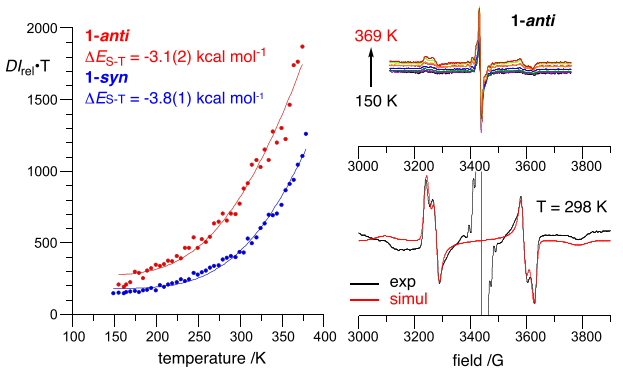

Figure 5. Left: $DI_{rel}T(T)$ data points and Bleaney−Bowers fitting for **1**-*anti* (red) and **1**-*syn* (blue). Right: VT EPR spectra in poly(2-isopropenyl-2-oxazoline) solid solutions of **1**-*anti* for selected temperatures (upper) and simulation of the triplet spectrum (red, lower) at 298 K: $|D/hc| = 0.033$ cm^{-1}, $|E/hc| = 0.0011$ cm^{-1}.

parameters obtained through simulation of the spectra indicate the proximity of the two spins (~4.3 Å) consistent with the molecular structures. Analysis of the relative intensity of the $|\Delta m_s| = 1$ signal, DI_{rel}, as a function of temperature, $DI_{rel}T(T)$, was performed using a modified Bleaney−Bowers formalism,[26,28] on the basis of Heisenberg Hamiltonian for a two electron system, $\hat{H} = -2J\hat{S}_1 \cdot \hat{S}_2$. This model gave a singlet−triplet gap, $\Delta E_{S\text{-}T}$, of **1**-*anti* and **1**-*syn*, −3.1(2) and −3.8(1) kcal mol^{-1}, respectively, although the high temperature data points could be affected by slow thermal equilibration of the *syn* and *anti* forms. The experimental $\Delta E_{S\text{-}T}$ values compare to −3.1 and −2.7 kcal mol^{-1} calculated for **1**-*anti* and **1**-*syn*, respectively, using the Yamaguchi broken-symmetry DFT formalism, and are consistent with the observation of a well resolved ^{1}H NMR spectrum of the **1**-*syn* isomer (but not **1**-*anti*) at −80 °C. The diradicaloid index[29] y_0 for both diradicals was calculated to be 0.86.

Both stereoisomers **1**-*syn* and **1**-*anti* exhibit similar two one-electron quasi-reversible oxidation processes separated by about 0.38 V (Table 1, Figure 6), and two-electron reduction. Stereoisomer **1**-*anti* undergoes more facile oxidation than the

Table 1. Results of Electronic Absorption[a] and DPV[b] Measurements for Blatter and Diradicals 1

radical	λ_{max} exp[a] (nm)	λ_{max} DFT[c] (nm)	$E_{1/2}^{-2/0}$ (V)	$E_{1/2}^{0/+}$ (V)	$E_{1/2}^{+/+2}$ (V)
Blatter[d]	492	474	−1.38	−0.18	
1-*anti*	678	790	−1.48	−0.21	0.18
1-*syn*	622	798	−1.47	−0.17	0.20

[a]Recorded in CH_2Cl_2. [b]Recorded in CH_2Cl_2 (0.5 mM). Conditions: $[n\text{-}Bu_4N]^+[PF_6]^-$ (0.1 M), glassy carbon electrode, scan rate 5 mV·s^{-1}, *ca.* 20 °C. Potentials *vs* Fc/Fc^+. For details, see the SI. [c]DFT calculated composite peak. See the SI. [d]Ref 27.

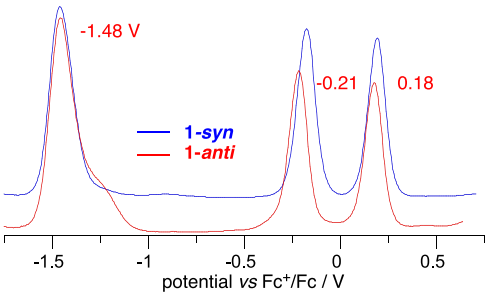

Figure 6. Differential pulse voltammograms (DPV) of diradicals **1**-*syn* (blue) and **1**-*anti* (red) in 0.1 M $[Bu_4N]^+PF_6^-$ in CH_2Cl_2 with indicated potentials for **1**-*anti*. Scan rate: 5 mV s^{-1}. For details, see the SI.

syn isomer and the prototypical Blatter radical[27] by about 0.03 V, which is due to particularly strong transannular $\pi-\pi$ interactions (π compression). These interactions are also responsible for the cathodic shift of the reduction process relative to that of the parent Blatter, and a large anodic shift of the second oxidation process due to delocalization and stabilization of the positive charge in the radical cation.

The observed large separation of the two oxidation processes should, in principle, allow for selective oxidation of the diradicals to the corresponding radical cations. Preliminary experiments demonstrated that treatment of a mixture of the two stereoisomers with an excess AgOTf in THF led to selective precipitation of the [**1**-*syn*][OTf] radical cation salt, while the *anti* isomer remained in the solution and underwent double oxidation to dication salt [**1**-*anti*][2OTf]. Interestingly, CF_3COOAg formed a complex with **1**-*syn* instead of oxidizing it, as demonstrated by XRD analysis.[26] Single crystal analysis of the two cations[26] revealed that the separation between the [1,2,4]triazinyl rings is greater than that in the corresponding diradicals, as evident from the N(1)···N(1) distance, which is 0.17 and 0.29 Å longer for the $[\mathbf{1}\text{-}syn]^{+\bullet}$ and $[\mathbf{1}\text{-}anti]^{2+}$, respectively. The electronic structure of the former appears to be a multisite π bond between the two heterocycles, rather than a one electron σ bond.[30] TD-DFT analysis predicts an intense absorption at about 1500 nm ($f \sim 0.1$) for the former solely due to the α-HOMO−α-LUMO transition.

In summary, we have demonstrated a simple one-step approach to OSS diradicals with a cofacial arrangement of two Blatter radicals on the *peri*-naphthalene scaffold. The diradicals form two stable diastereoisomers, *syn* and *anti*, of which the latter was separated into enantiomers with the estimated half-life of 139 min at 65 °C. The diradicals appear to exist in the closed shell form (π dimer) in the solid-state and open-shell singlet in solutions with the S−T gap of about −3.1 (*anti*) and

https://doi.org/10.1021/jacs.4c16500
J. Am. Chem. Soc. 2025, 147, 125−129

−3.8 (*syn*) kcal mol^{-1}. It is remarkable that despite significant π compression the Blatter radical subunits apparently do not dimerize. The π compression results in a large separation of oxidation potentials, nearly 0.4 V, allowing the isolation of one of the radical cations. Results indicate that such materials could constitute a new class of NIR dyes.

■ ASSOCIATED CONTENT

Supporting Information

The Supporting Information is available free of charge at https://pubs.acs.org/doi/10.1021/jacs.4c16500.

Full details of synthesis and characterization of diradicals, IR, VT-NMR, and UV−vis spectra, XRD, VT-EPR, and computational details and results (PDF)

Accession Codes

Deposition Numbers 2385486−2385491 contain the supplementary crystallographic data for this paper. These data can be obtained free of charge via the joint Cambridge Crystallographic Data Centre (CCDC) and Fachinformationszentrum Karlsruhe Access Structures service.

■ AUTHOR INFORMATION

Corresponding Author

Piotr Kaszyński − *Faculty of Chemistry, University of Łódź, 91403 Łódź, Poland; Center for Molecular and Macromolecular Studies, Polish Academy of Sciences, 90363 Łódź, Poland; Department of Chemistry, Middle Tennessee State University, Murfreesboro, Tennessee 37132, United States;* orcid.org/0000-0002-2325-8560; Email: piotr.kaszynski@cbmm.lodz.pl

Authors

Paulina Bartos − *Faculty of Chemistry, University of Łódź, 91403 Łódź, Poland;* orcid.org/0000-0003-0514-951X

Dominika Pomikło − *Center for Molecular and Macromolecular Studies, Polish Academy of Sciences, 90363 Łódź, Poland;* orcid.org/0000-0003-1297-8922

Kadin B. Sorenson − *Department of Chemistry, Middle Tennessee State University, Murfreesboro, Tennessee 37132, United States*

Oleksandr Hietsoi − *Department of Chemistry, Middle Tennessee State University, Murfreesboro, Tennessee 37132, United States;* orcid.org/0000-0003-0332-1064

Andrienne C. Friedli − *Department of Chemistry, Middle Tennessee State University, Murfreesboro, Tennessee 37132, United States*

Complete contact information is available at: https://pubs.acs.org/10.1021/jacs.4c16500

Notes

The authors declare no competing financial interest.

■ ACKNOWLEDGMENTS

This project was supported by the National Science Center (2020/38/A/ST4/00597) and National Science Foundation (REU-1852543 and MRI-1626549) Grants. The authors thank Aldair Avalos-Madera, Ewa Zawistowska, and Dr. Tomasz Cierpiał for technical assistance.

■ DEDICATION

In memory of Professor Josef Michl (1939−2024).

■ REFERENCES

(1) Abe, M. Diradicals. *Chem. Rev.* **2013**, *113*, 7011−7088.

(2) (a) *Diradicaloids* Wu, J., Ed.; Jenny Stanford, 2022. (b) Gopalakrishna, T. Y.; Zeng, W.; Lu, X.; Wu, J. From open-shell singlet diradicaloids to polyradicaloids. *Chem. Commun.* **2018**, *54*, 2186−2199.

(3) (a) Hu, X.; Wang, W.; Wang, D.; Zheng, Y. The electronic applications of stable diradicaloids: present and future. *J. Mater. Chem. C* **2018**, *6*, 11232−11242. (b) Müller, T. J. J.; Bunz, U. H. F. *Functional Organic Materials: Syntheses, Strategies and Applications*; Wiley-VCH, 2007.

(4) (a) Ni, Y.; Wu, J. Diradical approach toward organic near infrared dyes. *Tetrahedron Lett.* **2016**, *57*, 5426−5434. (b) Kamada, K.; Fuku-en, S.-i.; Minamide, S.; Ohta, K.; Kishi, R.; Nakano, M.; Matsuzaki, H.; Okamoto, H.; Higashikawa, H.; Inoue, K.; et al. Impact of diradical character on two-photon absorption: bis(acridine) dimers synthesized from allenic precursor. *J. Am. Chem. Soc.* **2013**, *135*, 232−241. (c) Sun, Z.; Ye, Q.; Chi, C.; Wu, J. Low band gap polycyclic hydrocarbons: From closed-shell near infrared dyes and semiconductors to open-shell radicals. *Chem. Soc. Rev.* **2012**, *41*, 7857−7889.

(5) Fukuda, K.; Nagami, T.; Fujiyoshi, J.; Nakano, M. Interplay between open-shell character, aromaticity, and second hyperpolarizabilities in indenofluorenes. *J. Phys. Chem. A* **2015**, *119*, 10620−10627.

(6) Zheng, Y.; Miao, M.-s.; Dantelle, G.; Eisenmenger, N. D.; Wu, G.; Yavuz, I.; Chabinyc, M. L.; Houk, K. N.; Wudl, F. A solid-state effect responsible for an organic quintet state at room temperature and ambient pressure. *Adv. Mater.* **2015**, *27*, 1718−1723.

(7) Ito, S.; Nagami, T.; Nakano, M. Diradical-character-based design for singlet fission of bisanthene derivatives: Aromatic-ring attachment and π-plane twisting. *J. Phys. Chem. Lett.* **2016**, *7*, 3925−3930.

(8) Rogers, F. J. M.; Norcott, P. L.; Coote, M. L. Recent advances in the chemistry of benzo[*e*][1,2,4]triazinyl radicals. *Org. Biomol. Chem.* **2020**, *18*, 8255−8277.

(9) Blatter, H. M.; Lukaszewski, H. A new stable free radical. *Tetrahedron Lett.* **1968**, *9*, 2701−2705.

(10) Pomikło, D.; Pietrzak, A.; Kishi, R.; Kaszyński, P. Bi-Blatter diradicals: Convenient access to regioisomers with tunable electronic and magnetic properties. *Mater. Chem. Front.* **2023**, *7*, 4928−4943.

(11) Dai, D.; Zhan, Q.; Shi, T.; Wang, D.; Zheng, Y. Spin characteristics in conjugated stable diradicals. *Chem. Commun.* **2024**, *60*, 8997−9006.

(12) (a) Barker, J. E.; Dressler, J. J.; Cardenas Valdivia, A.; Kishi, R.; Strand, E. T.; Zakharov, L. N.; MacMillan, S. N.; Gomez-Garcia, C. J.; Nakano, M.; Casado, J.; Haley, M. M.; et al. Molecule isomerism modulates the diradical properties of stable singlet diradicaloids. *J. Am. Chem. Soc.* **2020**, *142*, 1548−1555. (b) Sun, Z.; Zeng, Z.; Wu, J. Zethrenes, extended *p*-quinodimethanes, and periacenes with a singlet biradical ground state. *Acc. Chem. Res.* **2014**, *47*, 2582−2591.

(13) Gallagher, N. M.; Olankitwanit, A.; Rajca, A. High-spin organic molecules. *J. Org. Chem.* **2015**, *80*, 1291−1298.

(14) Rajca, A.; Mukherjee, S.; Pink, M.; Rajca, S. Exchange coupling mediated through-bonds and through-space in conformationally constrained polyradical scaffolds: calix[4]arene nitroxide tetraradicals and diradical. *J. Am. Chem. Soc.* **2006**, *128*, 13497−13507. and references therein.

(15) Izuoka, A.; Murata, S.; Sugawara, T.; Iwamura, H. Ferro- and antiferromagnetic interaction between two diphenylcarbene units incorporated in the [2.2]paracyclophane skeleton. *J. Am. Chem. Soc.* **1985**, *107*, 1786−1787.

(16) Han, H.; Zhang, D.; Zhu, Z.; Wei, R.; Xiao, X.; Wang, X.; Liu, Y.; Ma, Y.; Zhao, D. Aromatic stacking mediated spin-spin coupling in cyclophane-assembled diradicals. *J. Am. Chem. Soc.* **2021**, *143*, 17690−17700.

(17) Hewitt, P.; Shultz, D. A.; Kirk, M. L. Magnetic exchange coupling through the nonalternant cyclopentadienyl π-system of ferrocene. *Org. Lett.* **2021**, *23*, 8235−8239.

(18) Koivisto, B. D.; Ichimura, A. S.; McDonald, R.; Lemaire, M. T.; Thompson, L. K.; Hicks, R. G. Intramolecular π-dimerization in a 1,1′-bis(verdazyl)ferrocene diradical. *J. Am. Chem. Soc.* **2006**, *128*, 690−691.
(19) Shimizu, A.; Hayashida, M.; Ochi, Y.; Shiomi, D.; Sato, K.; Takui, T.; Shintani, R. Zwitterionic open-shell singlet diradical with solvent-dependent singlet-triplet energy gap. *Asian J. Org. Chem.* **2023**, *12*, e202300224.
(20) (a) Katoh, T.; Ogawa, K.; Inagaki, Y.; Okazaki, R. Syntheses and properties of (1,8-naphthylene)bispyridines and related pyridinium compounds. *Tetrahedron* **1997**, *53*, 3557−3570. (b) Kuroda, M.; Nakayama, J.; Hoshino, M.; Furusho, N.; Kawata, T.; Ohba, S. Synthesis and properties of 1,8-Di(2-thienyl)-, 1,8-bis(5,2′-bithiophene-2-yl)-, 1,8-bis(5,2′:5′,2″-terthiophene-2-yl)-, and 1,8-bis(5,2′:5′,2″:5″,2‴-quaterthiophene-2-yl)naphthalenes and related compounds. *Tetrahedron* **1993**, *49*, 3735−3748. (c) Feng, J.; Chen, X.; Han, Q.; Wang, H.; Lu, P.; Wang, Y. Naphthalene-based fluorophores: Synthesis characterization, and photophysical properties. *J. Lumin.* **2011**, *131*, 2775−2783. (d) Hu, J.-Y.; Pu, Y.-J.; Yamashita, Y.; Satoh, F.; Kawata, S.; Katagiri, H.; Sasabe, H.; Kido, J. Excimer-emitting single molecules with stacked π-conjugated groups covalently linked at the 1,8-positions of naphthalene for highly efficient blue and green OLEDs. *J. Mater. Chem. C* **2013**, *1*, 3871−3878. (e) Wolf, C.; Mei, X. Synthesis of conformationally stable 1,8-diarylnaphthalenes: Development of new photoluminescent sensors for ion-selective recognition. *J. Am. Chem. Soc.* **2003**, *125*, 10651−10658.
(21) (a) Trtica, S.; Prosenc, M. H.; Schmidt, M.; Heck, J.; Albrecht, O.; Görlitz, D.; Reuter, F.; Rentschler, E. Stacked nickelocenes: Synthesis, structural characterization, and magnetic properties. *Inorg. Chem.* **2010**, *49*, 1667−1673. (b) Pagels, N.; Albrecht, O.; Görlitz, D.; Rogachev, A. Y.; Prosenc, M. H.; Heck, J. Electronic coupling through intramolecular π−π interactions in biscobaltocenes: A structural, spectroscopic, and magnetic study. *Chem.—Eur. J.* **2011**, *17*, 4166−4176. (c) Hasegawa, M.; Daigoku, K.; Hashimoto, K.; Nishikawa, H.; Iyoda, M. Face-to-face dimeric tetrathiafulvalenes and their cation radical and dication species as models of mixed valence and π-dimer states. *Bull. Chem. Soc. Jpn.* **2012**, *85*, 51−60.
(22) (a) Tumambac, G. E.; Wolf, C. Synthesis and stereodynamics of highly constrained 1,8-bis(2,2′-dialkyl-4,4′-diquinolyl)-naphthalenes. *J. Org. Chem.* **2004**, *69*, 2048−2055. (b) Ghosn, M. W.; Wolf, C. Synthesis, conformational stability, and asymmetric transformation of atropisomeric 1,8-bisphenolnaphthalenes. *J. Org. Chem.* **2011**, *76*, 3888−3897.
(23) Constantinides, C. P.; Obijalska, E.; Kaszyński, P. Access to 1,4-dihydrobenzo[*e*][1,2,4]triazin-4-yl derivatives. *Org. Lett.* **2016**, *18*, 916−919.
(24) (a) Berezin, A. A.; Zissimou, G.; Constantinides, C. P.; Beldjoudi, Y.; Rawson, J. M.; Koutentis, P. A. Correction to route to benzo- and pyrido-fused 1,2,4-triazinyl radicals via *N*′ (Het)aryl *N*′ [2-nitro(het)aryl]hydrazides. *J. Org. Chem.* **2015**, *80*, 8943−8944. (b) Zissimou, G.; Manoli, M.; Koutentis, P. A. 3,3′-Diphenyl-1,1′-bis(pyridin-2-yl)-7,7′-bis(trifluoromethyl)-1′,4′-dihydro-1*H*-4,5′-bibenzo[*e*][1,2,4]triazin-4-yl. *CSD Commun.* **2023**, CCDC 2234327.
(25) Di Motta, S.; Negri, F.; Fazzi, D.; Castiglioni, C.; Canesi, E. V. Biradicaloid and polyenic character of quinoidal oligothiophenes revealed by the presence of a low-lying double-exciton state. *J. Phys. Chem. Lett.* **2010**, *1*, 3334−3339.
(26) For details, see the SI.
(27) (a) Pomikło, D.; Bodzioch, A.; Pietrzak, A.; Kaszyński, P. C(3) Functional derivatives of the Blatter radical. *Org. Lett.* **2019**, *21*, 6995−6999. (b) Pomikło, D.; Bodzioch, A.; Kaszyński, P. 3 Substituted Blatter radicals: Cyclization of *N*-arylguanidines and *N*-arylamidines to benzo[*e*][1,2,4]triazines and PhLi addition. *J. Org. Chem.* **2023**, *88*, 2999−3011.
(28) Bleaney, B.; Bowers, K. D. Anomalous paramagnetism of copper acetate. *Proc. R. Soc. London, Ser. A* **1952**, *214*, 451−465.
(29) (a) Yamaguchi, K.; Kawakami, T.; Takano, Y.; Kitagawa, Y.; Yamashita, Y.; Fujita, H. Analytical and *ab initio* studies of effective exchange interactions, polyradical character, unpaired electron density, and information entropy in radical clusters (R)N: Allyl radical cluster (N = 2−10) and hydrogen radical cluster (N = 50). *J. Quantum Chem.* **2002**, *90*, 370−385. (b) Döhnert, D.; Koutecký, J. Occupation numbers of natural orbitals as a criterion for biradical character. Different kinds of biradicals. *J. Am. Chem. Soc.* **1980**, *102*, 1789−1796.
(30) Shimajiri, T.; Kawaguchi, S.; Suzuki, T.; Ishigaki, Y. Direct evidence for a carbon-carbon one-electron σ-bond. *Nature* **2024**, *634*, 347−352.

https://doi.org/10.1021/jacs.4c16500
J. Am. Chem. Soc. 2025, 147, 125−129